Publication in the proceedings CD of the conference and Publication in the journal "Oxidation of Metals"

Atom Probe Tomography of Oxide Scales

K. Stiller[a], L. Viskari[a], G. Sundell[a], F. Liu[a], M.Thuvander[a], H-O Andrén[a], D.J. Larson[b], T. Prosa[b], D. Reinhard[b]

[a]*Chalmers University of Technology, Department of Applied Physics, 41296 Gothenburg, Sweden*
[b]*Cameca Instruments Inc. 5500 Nobel Drive Madison, WI 53711, USA*
stiller@chalmers.se

Abstract. Atom probe tomography, APT, is the only microstructural method that can routinely analyse and position individual atoms in a material with a spatial resolution of 0.1-0.5 nm. Recent implementation of pulsed-laser to APT made investigation of less conducting materials, such as oxides, feasible. In this paper a short description of the principle of the techniques is presented. It is followed by examples of recent APT studies of thermally grown oxide scales produced on alumina formers (Pt-modified NiAl diffusion coating and FeCrAl alloy), at the crack tips in a Ni-based alloy and on a Zr-alloy. Additionally results from preliminary studies of ZnO and MgO bulk materials are shown. The obtained information on the atomic scale about the chemistry variations in the scales and at the metal oxide interfaces provides valuable insights into oxidation processes.

Keywords: Atom probe tomography, oxides, microstructure, atomic scale.

INTRODUCTION

The degradation of materials by high temperature corrosion/oxidation is an important issue in many applications. It limits the useful life of installations, restricts the utilisation of the fuel and obstructs the development of more economical and environmentally friendly processes and systems. The degradation is controlled by the properties of the oxide scales that develop including oxide grain boundaries and oxide–metal interfaces. However, even if studied for many years, the processes behind the complex interplay between the oxide microstructure, ionic transport and oxidation kinetics are still not completely understood to large extent because of the lack of atomic scale information. We need to know where and how different species are situated.

Analytical techniques such as X-ray Photoelectron Spectroscopy (XPS) or Auger Electron Spectroscopy (AES) have too poor lateral resolution (μm-range) to fulfil this requirement. They also suffer from relatively poor detection limit (about 0.1 at%) and quite complex quantification of chemical analysis. Secondary Ion Mass Spectrometry (SIMS) allows for detection of very low amounts of elements (down to the ppb level in the case of dynamic SIMS) but the lateral resolution of this technique (sub-micrometre) does not really allow for atomic scale analysis. Moreover, as the secondary ion yield depends on the ionization energy, the quantification of the obtained results is not trivial.

Recent development of the methods for high-resolution microstructural studies opened new opportunities to improve our understanding of oxidation processes. The invention of focused ion beam (FIB) milling techniques created possibilities never seen before for almost routine preparation of thin foils, containing oxide scale and the underlying metal, for Transmission Electron Microscopy (TEM) studies. High resolution TEM has evolved into a versatile tool for detailed investigations at sub-nm level. Very recently, three-dimensional characterisation at the atomic scale has been demonstrated for special cases using a high angle annular dark field scanning TEM [1]. However, atom probe tomography (APT) is unbeatable in this respect: it is the only method that can routinely analyse and position individual atoms in a material with nearly atomic resolution and with an equal sensitivity for all the elements. In the past, the applications of atom probe technique had been limited to only conductive materials. Recent implementation of pulsed-laser to APT made investigation of less conducting materials, such as oxides, feasible.

In this paper we will first shortly describe basic the principles of APT technique including specimen preparation. Thereafter, we will show recent examples of the application of the method to studies of different oxide scales and bulk oxides.

APT BASIC PRINCIPLES

The three-dimensional atom probe technique, also called APT, can identify and position individual atoms in a material with a spatial resolution of 0.1-0.5 nm. In the conventional APT instrument, individual

atoms are field evaporated from needle-shaped specimens (<100 nm radius) using a high positive voltage. In principle, to perform atom probe analysis, the specimen is subjected to a positive standing voltage (~10 kV) to which short (a few nanoseconds) voltage pulses, with the amplitude typically 0.1 to 0.2 of the standing voltage, are added. The applied high electrical field (~10^{10} V/m) results in ionisation of the atoms at the specimen surface. This phenomenon, known as field evaporation [2], is essentially a thermally activated process. The produced ions are repelled by the specimen and eventually reach the position sensitive detector where their impact coordinates are recorded, thereby making reconstruction of the positions of the ions in the sample possible. The identity of the ions is determined with time-of-flight mass spectrometry. Consequently, the atomic-scale chemistry of the analysed sample volume is reconstructed in three dimensions. The depth to which an APT specimen can be analysed depends on the material and may exceed one micrometre. The detection sensitivity is less than 10 atomic parts per million, with the standard error being determined mainly by counting statistics. Thus, APT is an important tool for characterisation of chemistry at different types of interfaces, nanometre-sized precipitates and thin multilayers structures.

Due to the inability of samples of low electrical conductivity to transmit the pulses, the use of voltage pulsing in the conventional instruments limited the applications of the technique to materials with an electrical conductivity greater than 100 S/cm i.e. to metals and heavily doped semiconductors. However, recent implementation of pulsed-laser technique to APT made almost routine investigations of semiconductors and dielectrics possible [3]. Whereas an application of APT to semiconductor research is quite well established, investigation of thermally grown or bulk oxides using APT still remains an unexplored field. In pulsed-laser instruments, the field evaporation is generated by fast (<10 ps) laser pulses superimposed onto the standing voltage on the sample. The mechanism by which laser-induced evaporation of atoms takes place was until recently a subject of scientific debate. It is now generally accepted that in the case of metals, evaporation originates from heating of the specimen surface, since the absorbed light generates a transient increase in the surface temperature [4]. A similar explanation works even for semiconductors but cannot explain field evaporation of large band gap dielectrics such as ZrO_2, MgO and Al_2O_3 caused by low energy photons. It has recently been proposed that the mechanism responsible for field evaporation in such materials is the generation of holes at the surface of the investigated sample, which would substantially reduce the activation barrier height for field evaporation. Also the large relative surface of the tiny sample will induce more numerous surface states within the band gap, possibly aiding in absorbing the laser energy [5, 6]. It has been demonstrated that several oxides (ZrO_2-$MgAl_2O_4$, MgO, TiO_2 etc.) could be successfully analysed by APT using UV laser [6,7] but it was stated that the technique should not work for the visible light. However, the successful APT analyses of Al_2O_3 using of 532 nm pulsed laser show the opposite [8,9]. In this paper we will demonstrate the applicability of green laser APT for investigations of several large band- gap oxides.

Specimen Preparation

Specimen preparation is of crucial importance for APT studies. In the past electropolishing methods have been used to fabricate sharp needles from whiskers, wires or blanks, cut from bulk material [10]. However, such an approach is not possible for preparation of non-conducting specimens.

With the invention of focused ion beam milling (FIB) and its application to fabrication of both thin foils for TEM and APT specimens, the situation has dramatically improved. The method relies on sputtering of material with high precision so that a specimen with a desired shape and at a specific location is produced. Today FIB is extensively used for preparation of APT specimens from multilayer and surface films, semiconductor devices and also for producing site-specific metallic specimens [10]. The method is also suitable for preparation of thermally grown oxides. Fig. 1 a shows a piece of micro-sample cut from an oxidized NiAl diffusion coating (see the text below) that was lifted out and soldered on the top of a pre-prepared silicon post. Fig. 1b shows the final shape of this APT specimen that was obtained using annular milling.

EXPERIMENTAL

APT analyses of thermally grown oxide scales produced on alumina formers (Pt- modified NiAl diffusion coating and FeCrAl alloy), at the crack tips in Ni-based alloy and on Zr-alloy were conducted. Additionally preliminary studies of ZnO and MgO bulk materials were undertaken. Investigations were performed on Imago LEAP instruments (straight flight-path 3000X Si in investigations of NiAl and reflectron 3000X HR in the remaining studies) using green laser (532 nm) with 10 ps pulses. The diffusion coating specimens were held at a temperature of 20 K during analyses while studies of the remaining materials were performed at 70-85 K. The energy of the laser pulses was different for different materials and varied from 0.05 nJ for ZnO to 0.5 nJ in the case of FeCrAl. Reconstructions of acquisitions were done

using Imago IVAS software. Site-specific sample preparation of APT samples was performed on a FEI Strata 235 combined FIB and Scanning Electron Microscope (SEM) instrument using Ga ions.

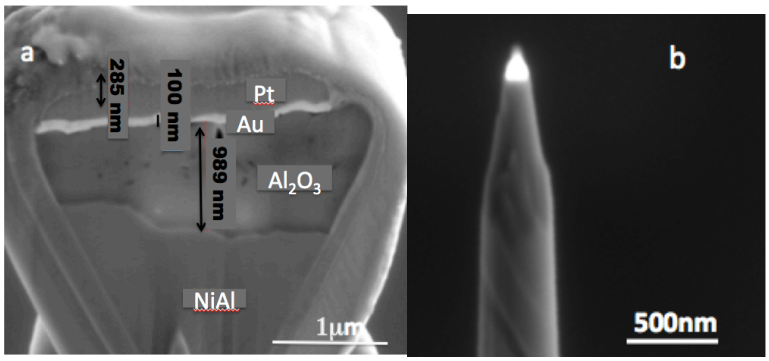

FIGURE 1. a) Piece of micro-sample cut from oxidized NiAl diffusion coating using FIB **b)** Final shape of the APT specimen obtained using annular milling.

APPLICATIONS

Analyses of Al_2O_3 Formers

Crystalline alumina is an insulator with a band gap of about 8 eV and for a ceramic material quite high thermal conductivity ($30 Wm^{-1}K^{-1}$). The last mentioned property is theoretically beneficial for a good mass resolution in laser-pulsed APT because it will promote fast transport of thermal pulses in the material. The alumina scale is formed at high temperatures on Al- containing Ni- base (NiAl, NiCrAl, NiCrAlY) and Fe base (FeAl, FeCrAl, FeCrAlY) alloys and and is treated as protective because it is dense and slow-growing. Al_2O_3 is therefore one of the most important oxides to study to obtain better understanding of oxidation of high temperature materials.

Scale Formed on Pt-Modified NiAl Diffusion Coating

NiAl alloys are being extensively used at high temperatures as oxidation-resistant coating materials since they create a protective α-Al_2O_3 scale through selective oxidation of Al. The oxidation resistance of the coating may be further improved using different alloying additions. However, the exact mechanisms behind such improvements are not always fully understood mainly due to the lack of information about the microstructure of the created oxide scale on an atomic scale. Here we report about the first APT analyses of the oxide scale formed on a Pt-modified NiAl coating, MDC150L (Thermatech, USA), investigated after an exposure of 200 h at 1050°C in air [11]. The typical matrix composition of the coating, close to the surface, in the as-coated condition is 48.8Ni-40.1Al-5.1Co-2.2Cr -3.7Pt in at%.

APT analysis reveals the existence of very small (few nm in size) precipitates in the metal below the oxide scale, Fig. 2a. In this figure the oxide scale is represented by O ions while the underlying metal is represented by Ni ions. The Cr-rich precipitates consist of about 80 at% Cr and 10 at% Al. The concentration profiles through the precipitates and the oxide metal interface, Fig. 2, show some oxygen penetration into the precipitates from the oxide side. This is however not a real effect, but an artefact associated with the evaporation processes at this interface (see also the discussion below).

Figure 3 shows an APT mass spectrum of the oxide scale. Its mass resolving power ($m/\Delta m$) is relatively good, 182 at full width half maximum. In contrast to what is observed in the mass spectra from the underlying metal, it contains many oxide molecular ions, such as AlO^{2+}, $Al_2O_3^{+}$, AlO^{+} and AlO_2^{+}. This is indicative for APT analyses of oxides. Based on this data it was found that the oxide is a very pure alumina with around 39 at% Al, 61 at% O with practically no Cr (<0.1 at%) or any other element. No signs of any uneven distribution of Al, O or any other element in the oxide were detected. Keeping in mind the often alleged high solubility of Cr in alumina and the presence of Cr-rich precipitates and in the underlying metal, the absence of Cr in the oxide deserves some comments. Contrary to what is observed in the case of FeCrAl alloy exposed to 900° C (see below), Cr–rich particles were not observed in the oxide scale. It is therefore most likely that the Cr-rich precipitates dissolve when they are reached by the inward growing oxide, and that the excess of Cr is incorporated into the precipitates in the metal below the oxide. The metal-oxide interface was quite sharp with a less than 5 nm oxygen diffusion zone into the metal. No signs of segregation of any element to this interface could be observed.

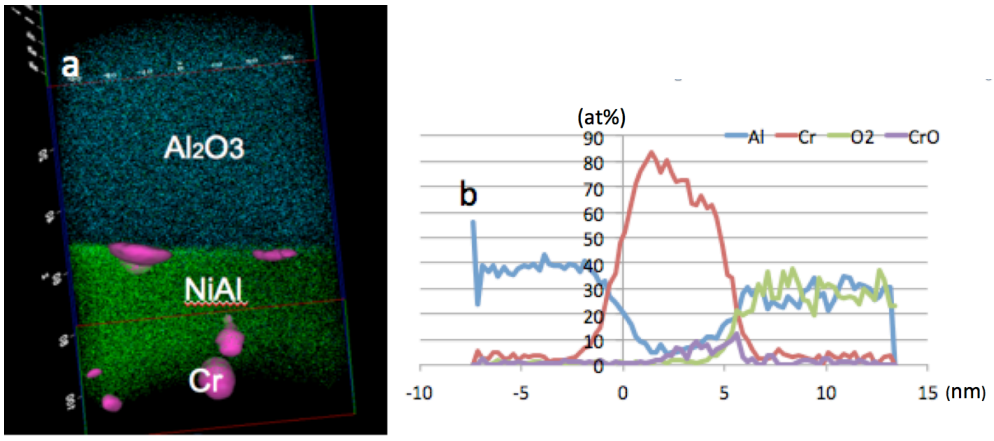

FIGURE 2. a) 3D reconstruction of the oxidised Pt-modified NiAl diffusion coating. Oxide represented by O ions (blue dots); metal by Ni (green); Cr-rich precipitates in purple. The box size is 50x50x100 nm^3 **b)** Compositional profile across the Cr-rich precipitate at the oxide–metal interface: x-axis distance (nm); y-axis concentration (at%)(interface at 0).

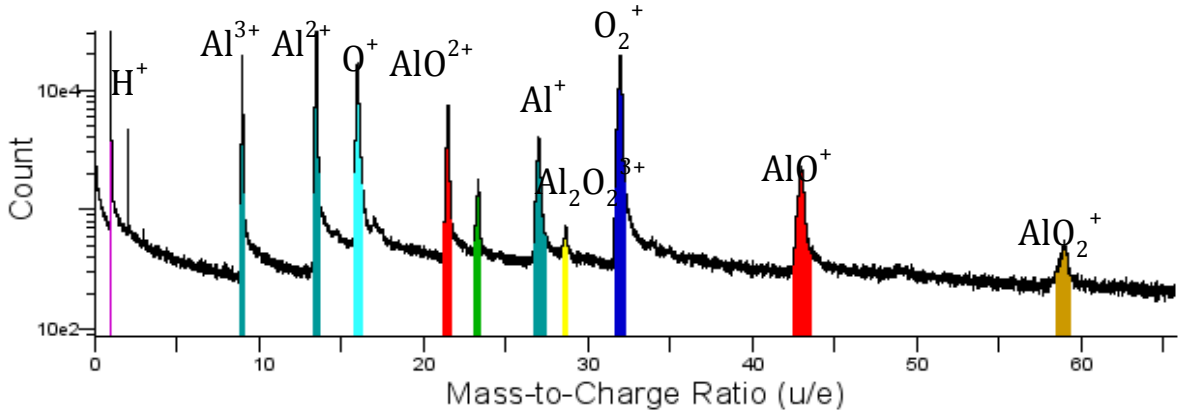

FIGURE 3. APT mass spectrum of the oxide scale formed on a Pt-modified NiA diffusion coating.

Scale Formed on a FeCrAl Alloy

FeCrAl alloys have outstanding oxidation resistance at very high temperatures (~1200°C), where they can be used as, for instance, heating elements in furnaces. They can also be applied in a relatively low temperature regime (300-900°C) as, for example, carrier material for catalyst converters in exhaust systems of automobiles. At high temperatures around 1000°C a dense, continuous, adherent and slow-growing α-Al_2O_3 scale form on the alloys. At temperatures <1000°C, relatively little information is available on the oxidation properties. To some extent, this can be attributed to the difficulty in characterizing very thin oxide scales (often <1 μm), which necessitates the use of techniques with high spatial resolution and/or high surface sensitivity. We have previously performed a series of studies of the alloy that was exposed to different environments (dry and humid air) by using SIMS, AES, SEM, and TEM [12-15]. The studies revealed that there is a Cr-rich layer in the middle of the oxide scale, above the α-alumina layer adjacent to the metal. It was concluded that this Cr-rich layer marks the original sample surface. No segregation of any element to the oxide metal interface was observed.

Here we show that, although challenging, APT has a great potential to provide valuable information for understanding oxidation of FeCrAl at relatively low temperatures. We studied thermally grown Al_2O_3 on a Rapidly Solidified Powder (RSP) metallurgical FeCrAl alloy, Kanthal APMT. The chemical composition of the alloy is 22 Cr, 5 Al, 3 Mo, 0.7 Si, 0.4 Mn in wt% and trace amounts of Y, Zr, Hf, C, Ti, Ni, Mg, and N (balance Fe). To simulate the boiler environment with low oxygen

concentration, the alloy was exposed to 5 vol.% O_2 + 95 vol.% N_2 at 900°C for 1 hour. TEM and XRD studies of the oxide scale reveal

Figure 4 shows a 3-D reconstruction of a volume consisting of 3 million ions, and with both the Al_2O_3 scale and the substrate metal. The small blue dots represent O ions, thus outlining the oxide. Only 10% of the total O ions are shown for visual clarity. The green spheres represent Ni ions. Notice that there is Ni segregation at the oxide/metal interface (0.2 at.% compared to < 0.04 at.% the metal matrix). The enrichment of Ni at the interface expressed in terms of its excess at the interface per area is 0.8 nm^{-2}. Cr-enriched nano-sized particles were detected inside the alumina scale. One of these particles is represented in Figure 4 by an iso-concentration surface of 8 at.% Cr (in magenta). The small size of the precipitates makes them difficult (if not impossible) to detect by other techniques. Two different populations of the precipitates were observed: one Fe-rich and the other Fe-poor (see figure 4 b). The oxygen content in the precipitates was high, around 30 at.%. Investigation of the same FeCrAl alloy exposed at 1100° C for 168 h revealed a very pure alumina scale with no Cr precipitates. The last result is consistent with that obtained from ~~the~~ analysis of Pt-modified NiAl coatings which showed that alumina scales formed at temperatures above 1000°C are free from impurities.

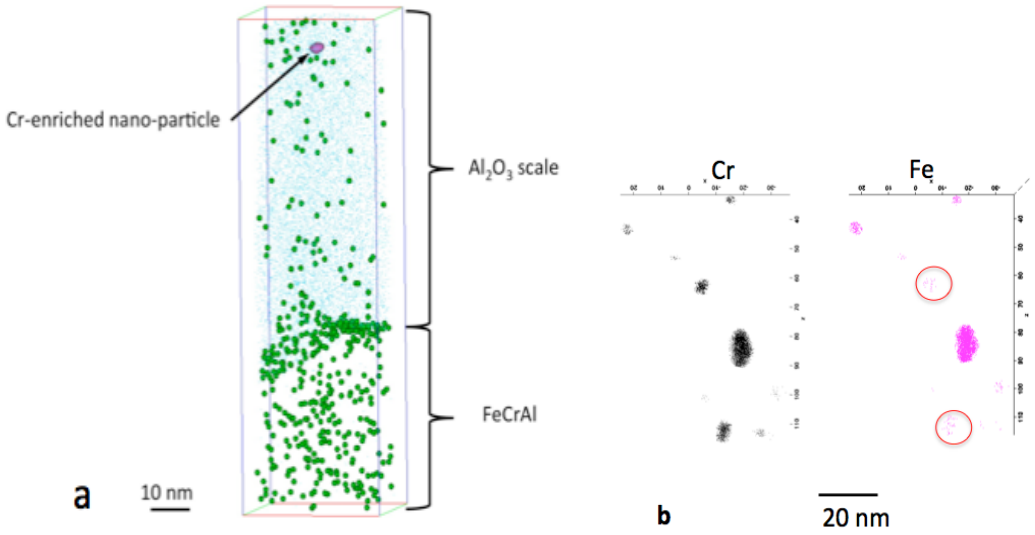

FIGURE 4. a) Projection of a 3-D reconstruction of Al_2O_3 oxide scale and the substrate FeCrAl alloy. The light-blue dots represent O ions (only 10% are shown for visual clarity). It outlines the oxide/metal interface. The green spheres represent Ni ions. Segregation of Ni to oxide / metal interface clearly visible. The magenta surface represents the 8 at.% Cr iso-concentration surface. It shows a Cr-enriched nano-particles ~5 nm. b) Another 3-D reconstruction showing distribution of Cr (black) and Fe (magenta) in the oxide scale. Circles indicate Fe-poor precipitates.

APT of Oxides at Crack Tips in Ni-based Alloys

Oxygen-rich environments are known to promote intergranular time-dependent crack growth in superalloys when these are subjected to a high temperature sustained load or certain fatigue cycles. It is believed that the quality of the oxide formed at the tip of the propagating crack is one of the important factors in the degradation of these materials.

APT was used for detailed studies of local chemistry and microstructure variation at the crack tips of a Ni-based alloy containing 50.9 at% Ni, 20.3 Cr, 9.9 Fe, 9.5 Co, 3.3 Nb, and 3.4 Al, as major elements. The pre-cracked specimens were exposed to a tensile load of 4 kN for 600 s at 700 °C in a controlled O_2 atmosphere. APT specimens were prepared using the method described in [16].

Fig 5 shows an APT reconstruction of the volume where the interface between the oxide scale at the crack tip (right part of the figure) and the adjacent unoxidized metal (left part) is present. Black dots represent the distribution of Fe ions, green of CrO_2 ions, blue of NiO ions and red of FeO ions. The uneven distribution of Fe in the left part of the figure reflects the presence of $Ni_3(Al,Nb)$ γ' phase precipitates in the metal matrix. According to APT analysis the γ' phase precipitates are low in Fe (1.3 at.% in γ' as compared to 13 at.% in the matrix) and therefore appear greyish. It is evident from the right part of the figure, i.e. the oxide part, that these precipitates oxidize differently from the

surrounding matrix. The oxide formed on the precipitates (light-blue areas) is almost pure NiO while the matrix forms $Ni(Fe,Cr)_2O_4$ spinel (dark blue areas). Cr is pushed away during oxidation and forms a Cr-rich M_2O_3 oxide (green area) close to the unoxidized metal. Below this oxide, an approximately 20 nm long oxygen enriched region with up to 2 at% O was found. A more detailed description of this study can be found elsewhere [16].

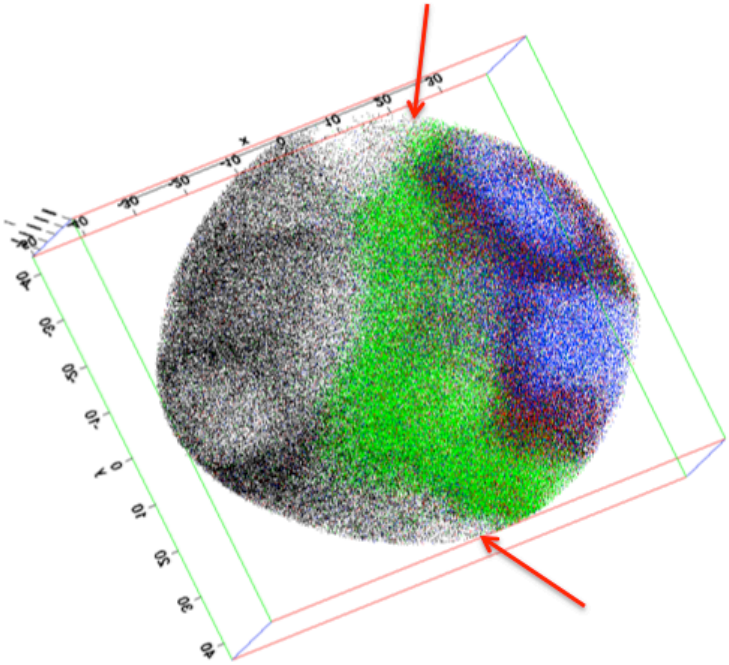

FIGURE 5. 3D reconstruction showing different oxide phases (green, blue and light-blue dots) at the crack tip and the unoxidized metal (black dots) Arrows indicates border between the oxidised and unoxidised material. The size of the box is 100x80x80 nm^3.

APT of Oxide Scale on Zr-alloy

Zirconium alloys are used in the nuclear industry as their small thermal neutron capture cross-section prevents the materials from interfering with the reactor neutron flux. The in-reactor lifetime is limited by waterside corrosion at high temperatures (270-340 °C) and pressures (7-15 MPa). The ZrO_2 oxide scale that forms grows inwards and is limited by O diffusion through a barrier layer of 1-2 µm. The Pilling-Bedworth ratio for zirconia is 1.56, resulting in stresses being built-up during the oxide growth. These are relieved by deformation of the underlying metal and by cracking of the oxide. This leads to cyclic oxide growth behaviour, where layers of dense oxide are separated by lateral cracks and voids. The materials in this study (Zircaloy-2, Zr-1.32 Sn - 0.17 Fe - 0.10 Cr - 0.05 Ni) were corroded in a static steam autoclave (10.3 MPa water vapour at 400°C for 72 h) in order to simulate conditions in a boiling water nuclear reactor. APT of the metal-oxide interface reveals that the oxygen content in the lower regions of the oxide is sub-stoichiometric. Finger-like features with higher O content stretch towards the metal, indicating that a mixture of phases exist Fig 6. The composition of the oxide in this region varies, and the O concentration is between 45-60 at%.

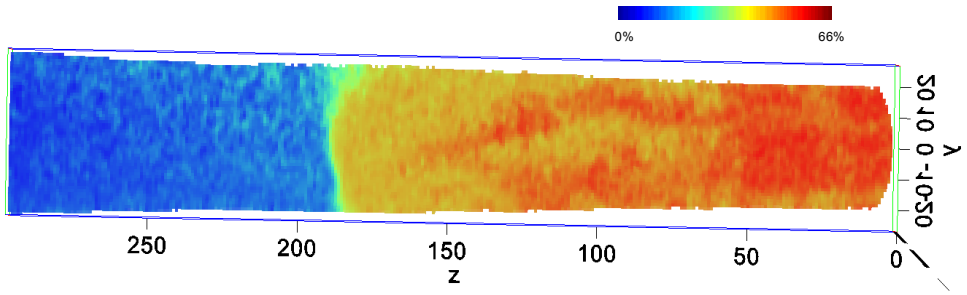

FIGURE 6. Atom probe reconstruction of local oxygen concentration at the metal-oxide interface in

Zircaloy. Blue corresponds to low concentrations and red to stoichiometric (66%) oxygen content in ZrO_2. The size of the area is 300x50 nm^2.

A sub-oxide phase with a thickness of 20-50 nm sometimes develops during the oxidation process, Fig 7. It contains approximately 30 at.% oxygen and is situated between the mixed oxide phase and the metal. It appears to have a significant effect on the oxygen ingress in the underlying metal, as diffusion profiles decreases abruptly in the presence of the sub-oxide whereas the profile stretches for several hundred nanometres before it reaches a base level in the material in the cases where no sub-oxide exists.

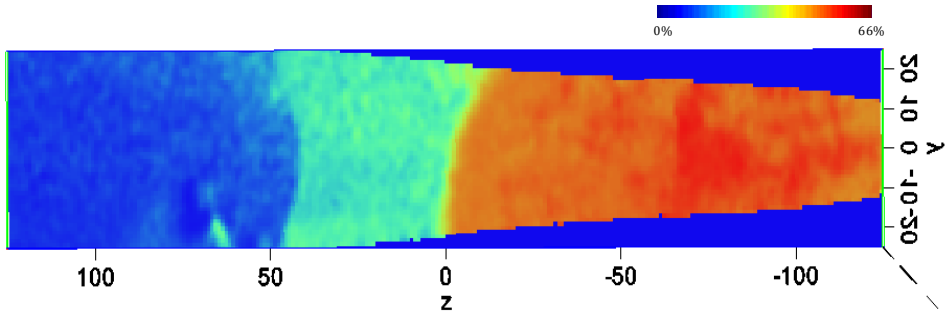

FIGURE 7. Atom probe reconstruction of the sub-oxide phase in Zircaloy. Blue corresponds to low concentrations and red to stoichiometric (66%) oxygen content in ZrO_2. The size of the area is 250x50 nm^2.

APT examination of the oxide also yields information about the distribution of alloying elements in zirconia, Fig 8. It is possible to observe segregation on a very small scale, which is extremely difficult to detect with electron microscopy. Minor segregation of Fe to an oxide grain boundary near the interface can be seen. This may have implications for the transport properties of the zirconia scale. Clearly, oxide microstructures and their implications for the corrosion mechanisms may be understood on an atomic scale.

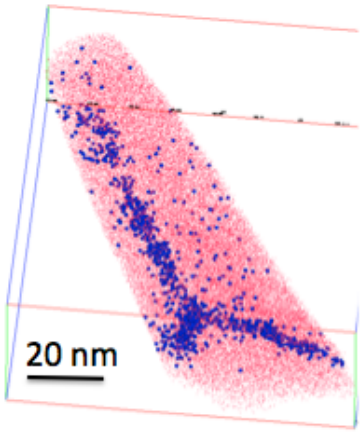

FIGURE 8. Segregation of Fe in ZrO_2. Blue spheres represent individual Fe atoms in the oxide.

APT of MgO and ZnO

In addition to oxide scales, it is also possible to analyse bulk oxides using laser pulsed APT. Figure 9 shows mass spectra from analyses of MgO and ZnO. The interpretation of the peaks is straightforward. The peaks have rather significant tails on the right side, towards higher mass-to-charge-state ratios. This is most probably caused by poor thermal conductivity, resulting in ions being field evaporated relatively long after the laser pulse. The presence of the tails possesses some difficulty when performing quantitative evaluation. In the case of ZnO, there is an unfortunate overlap between O^{2+} and Zn^{2+} at 32 Da. Even though this peak is by far the largest, the composition can still be obtained using the minor isotopes of Zn.

It has previously been shown that the quality of analysis is significantly improved when going from green to UV laser [17]. The analyses presented here were obtained using green laser, and shows that also

green laser can be used to get decent results. It is important to use correct experimental parameters, in particular the laser pulse energy. In the analysis of ZnO, a very poor mass spectrum was obtained when the laser energy was 0.2 nJ. Using 0.05 nJ, the result improved dramatically. This is probably directly related to the relatively poor thermal conductivity of ZnO. For MgO a laser pulse energy of 0.3 nJ could be used, thanks to the much better thermal conductivity (similar to that of Al_2O_3).

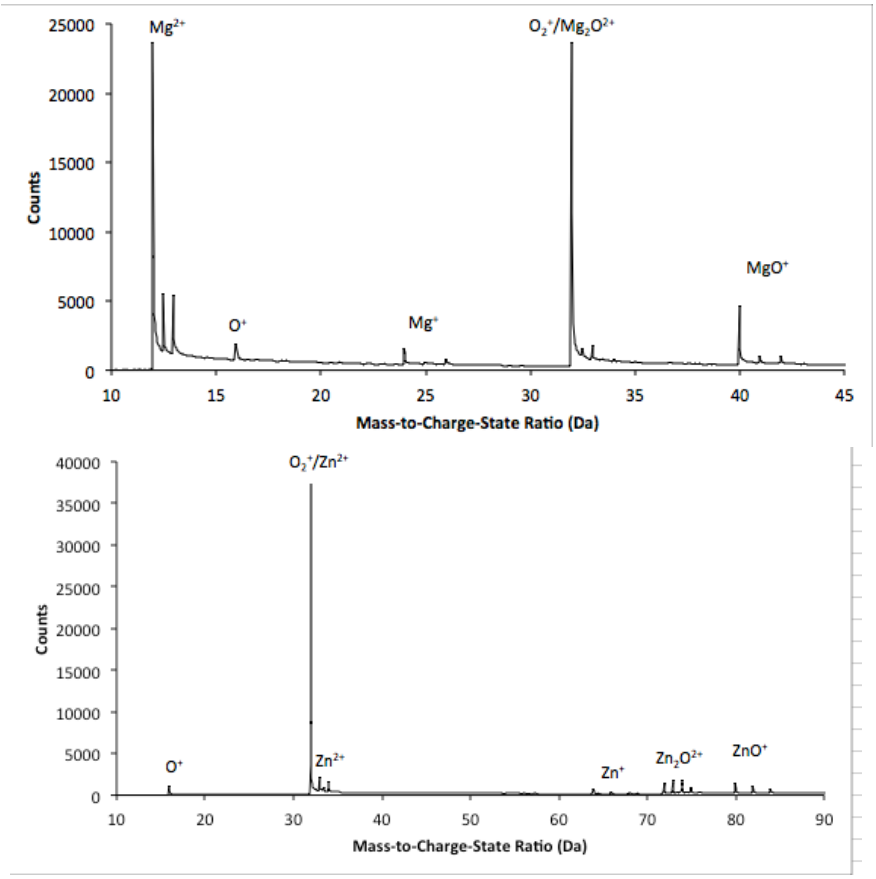

FIGURE 9. APT mass spectra from analyses of bulk MgO and ZnO.

SUMMARY

We have demonstrated the feasibility of analysing a wide variety of oxide scales using pulsed-laser APT. The obtained information on the atomic scale about the chemistry variations in the scales and at the metal oxide interfaces provides valuable insights into the oxidation processes. Thus "the realm of oxides" is now open for investigations using APT. The presented work also proves that green laser can be used for APT investigations of large-band gaps dielectrics indicating that the band gap of the investigated material is reduced by some mechanisms (surface states, impurities, sample preparation).

REFERENCES

1. S. Van Art, K. Batenburg, M.D. Rossell, et al., *Nature Letter*, **470,** 375 (2011)
2. E. W. Müller, J.A. Panitz and S.B. McLane, *Rev. Sci. Instrum*. **39** (1), 83 (1968)
3. A Renaissance in Atom-probe tomography, *MRS Bulletin* **34,** 717 (2009)
4. G. L. Kellogg and T. T. Tsong: *J. Appl. Phys*., **51**, 1184 (1980)
5. M. Tsukada, H. Tamura, K.P. McKenna et al. *Ultramicroscopy* **111**, 567 (2011)
6. A. Vella, B. Mazumder, G. Da Costa et al., *J. Appl. Phys.,* **110**, 044321 (2011)
7. K. Hono, T. Ohkubo, Y.M. Chen et al., *Ultramicroscopy* **111**, 576 (2011)
8. D.J. Larson, R.L. Alvis, D. F. Lawrence, *Microsc. Microanal*. **14** (suppl) 1254 (2008)
9. E.A. Marquis, N.A. Yahya, D. Larson et al., *Mater. Today*, **13** 34 (2010)

10. T.F. Kelly and M.K. Miller, Rev. Sci. Instr., **78**, 031101 (2007)
11. J. Angenete and K. Stiller, *Surf. Coat. Technol.,* **150**, 107 (2002)
12. H. Götlind, F. Liu, J.-E. Svensson, M. Halvarsson, L.-G. Johansson, *Oxid. of Metal.*, **67**, 251 (2007)
13. H. Josefsson, F. Liu, J.-E. Svensson, et al., *Materials and Corrosion*, 56 (2005) 801-805.
14. F. Liu, H. Götlind, J.-E. Svensson, et.al., *Corr. Sci.,* **50,** 2272 (2008).
15. F. Liu, H. Josefsson, J.-E. Svensson, et al. , *Materials at High Temperatures*, **22,** 521 (2005).
16. L. Viskari *PhD Thesis*. Department of Applied Physics Chalmers University of Technology 2011, ISBN: 978-91-7385-595-2
17. Y.M. Chen, T. Ohkubo and K Hono *Ultramicroscopy* **111**, 562 (2011)